



OPEN ACCESS

Original research

Off-label in-silico flow diverter performance assessment in posterior communicating artery aneurysms

Michael MacRaidl ,^{1,2,3} Ali Sarrami-Foroushani,^{1,4} Shuang Song,⁵ Qiongyao Liu ,⁵ Christopher Kelly,⁵ Nishant Ravikumar,⁵ Tufail Patankar,⁶ Toni Lassila,⁵ Zeike A Taylor ,⁷ Alejandro F Frangi ,^{1,3,4,8,9}

► Additional supplemental material is published online only. To view, please visit the journal online (<https://doi.org/10.1136/jnis-2024-022000>).

¹Centre for Computational Imaging and Modelling in Medicine (CIMIM), University of Manchester, Manchester, UK

²EPSRC Centre for Doctoral Training in Fluid Dynamics, University of Leeds, Leeds, UK

³Department of Computer Science, School of Engineering, University of Manchester, Manchester, UK

⁴School of Health Sciences, Division of Informatics, Imaging and Data Sciences, University of Manchester, Manchester, UK

⁵School of Computing, University of Leeds, Leeds, UK

⁶Interventional Neuroradiology, Leeds Teaching Hospitals NHS Trust, Leeds, UK

⁷School of Mechanical Engineering, University of Leeds, Leeds, UK

⁸Department of Cardiovascular Sciences, KU Leuven, Leuven, Belgium

⁹Department of Electrical Engineering (ESAT), KU Leuven, Leuven, Belgium

Correspondence to

Professor Alejandro F Frangi; alejandro.frangi@manchester.ac.uk

Received 18 May 2024

Accepted 13 September 2024



Check for updates

© Author(s) (or their employer(s)) 2024. Re-use permitted under CC BY-NC. No commercial re-use. See rights and permissions. Published by BMJ.

To cite: MacRaidl M, Sarrami-Foroushani A, Song S, et al. *J NeuroIntervent Surg* Epub ahead of print: [please include Day Month Year]. doi:10.1136/jnis-2024-022000

ABSTRACT

Background The posterior communicating artery (PCoMA) is among the most common intracranial aneurysm locations, but flow diverter (FD) treatment with the widely used pipeline embolization device (PED) remains an off-label treatment that is not well understood. PCoMA aneurysm flow diversion is complicated by the presence of fetal posterior circulation (FPC), which has an estimated prevalence of 4–29% and is more common in people of black (11.5%) than white (4.9%) race. We present the FD-PCoMA in-silico trial (IST) into FD treatment performance in PCoMA aneurysms. ISTs use computational modeling and simulation in cohorts of virtual patients to evaluate medical device performance.

Methods We modeled FD treatment in 118 virtual patients with 59 distinct PCoMA aneurysm anatomies, using computational fluid dynamics to assess post-treatment outcome. Boundary conditions were prescribed to model the effects of non-fetal and FPC, allowing for comparison between these subgroups.

Results FD-PCoMA predicted reduced treatment success in FPC patients, with an average aneurysm space and time-averaged velocity reduction of 67.8% for non-fetal patients and 46.5% for fetal patients ($P<0.001$). Space and time-averaged wall shear stress on the device surface was 29.2 Pa averaged across fetal patients and 23.5 Pa across non-fetal ($P<0.05$) patients, suggesting FD endothelialization may be hindered in FPC patients. Morphological variables, such as the size and shape of the aneurysm and PCoMA size, did not affect the treatment outcome.

Conclusions FD-PCoMA had significantly lower treatment success rates in PCoMA aneurysm patients with FPC. We suggest that FPC patients should be treated with an alternative to single PED flow diversion.

INTRODUCTION

Posterior communicating artery (PCoMA) aneurysms are among the most common intracranial aneurysm locations, accounting for 25% of all aneurysms.¹ Despite this, the most widely used flow diverter (FD), the pipeline embolization device (PED, Medtronic, Minneapolis, Minnesota, USA), is not approved by the US Food and Drug Administration (FDA, Silver Spring, Maryland, USA) for use in PCoMA aneurysms.² Flow diversion aims to promote stasis induced thrombosis in the aneurysm sac and endothelial proliferation of the

WHAT IS ALREADY KNOWN ON THIS TOPIC

⇒ Flow diverter (FD) treatment of posterior communicating artery (PCoMA) aneurysms using the pipeline embolization device (PED) is an off-label indication with poorly understood low treatment success rates in patients with fetal posterior circulation (FPC).

WHAT THIS STUDY ADDS

⇒ The FD-PCoMA in-silico trial used computer modeling and simulation in 118 virtual patients to determine that PED treatment of PCoMA aneurysms was less effective in patients with FPC and was due to the increased flow rate through the PCoMA in this scenario.
⇒ Morphological variables, such as PCoMA size, aneurysm maximum diameter, aneurysm aspect ratio, aneurysm neck width, and aneurysm non-sphericity index did not influence treatment outcomes.

HOW THIS STUDY MIGHT AFFECT RESEARCH, PRACTICE OR POLICY

⇒ Alternative treatment to single PED flow diversion is recommended for PCoMA aneurysms with FPC.
⇒ This study highlights how in-silico trials can generate evidence on medical device performance in less studied treatment scenarios.

neointima along the device itself, ultimately leading to aneurysm occlusion. Neointimal proliferation can also lead to parent vessel remodelling, which led to concerns that the PED has the potential to occlude side branches.³ Studies since have consistently found no neurological deficits following the treatment (ie, the safety of the treatment has been demonstrated), but efficacy in the presence of fetal posterior circulation (FPC) remains unclear.^{3–6}

FPC is defined by the absence (true fetal) or atrophy (fetal-type) of the P1 segment of the posterior cerebral artery (PCA).⁷ In these scenarios, the PCoMA provides some or all of the blood supply to the P2 PCA. The increased demand on the PCoMA leads to increased flow rates and potentially subsequent PCoMA hypertrophy, both of which could influence PED performance in the treatment of PCoMA aneurysms (see online supplemental figure 1 for images of exemplar non-fetal and fetal

vasculature for two patients from the @neurIST database⁸). FPC incidence is 4–29% unilaterally and 1–9% bilaterally,¹ it is more common in patients with PComA aneurysms than in those without,⁹ and it is more prevalent in patients of black (11.5%) than white (4.9%) race.¹⁰

Multiple case studies suggest treating fetal-type PComA aneurysms with alternative methods to the PED.^{11,12} A retrospective review of 49 patients by Rinaldo *et al*⁶ found that PED occlusion rates were 43.7% for patients with fetal PComA aneurysms and 81.8% for patients without FPC. Rinaldo *et al* defined FPC as a PComA diameter greater than that of the P1 PCA. Increased flow rates are also a characteristic of FPC, which poses the question of whether it is the increased PComA diameter or the increased flow that hinders PED treatment.¹³

Prospective clinical trials into PED treatment have not focused on PComA aneurysms to date. The PUFs (Pipeline for Uncoilable or Failed Aneurysms¹⁴), PREMIER (Prospective Study on Embolization of Intracranial Aneurysms With Pipeline Embolization Device¹⁵), and ASPIRe (Aneurysm Study of Pipeline in an Observational Registry¹⁶) prospective clinical trials into PED flow diversion collectively contained 23/456 (5.0%) PComA aneurysms. The IntrePED (International Retrospective Study of the Pipeline Embolization Device¹⁷) retrospective study contained 61/906 (6.7%) PComA aneurysms. None of these studies reported specific findings for PComA subgroups. PComA aneurysms with FPC have similarly not been specifically reported on in large-scale clinical trials.

In clinical trials, some treatment scenarios may be unfeasible or unethical to impose in real life patients, and demographic biases due to study type, location, or other selection criteria (eg, age) may be unavoidable.¹⁸ In-silico trials (ISTs), which use computational modelling and simulation in cohorts of virtual patients, can provide insights into medical device performance in scenarios that are difficult to assess in clinical trials and/or in demographics that may be less well represented. In-silico methodologies are being adopted for drug and medical device development¹⁹ in the treatment of various pathologies, such as intracranial aneurysms,²⁰ acute ischemic stroke,²¹ and COVID-19.²² Previous work has established that ISTs for flow diversion of intracranial aneurysms can replicate and expand on results from clinical trials of intracranial aneurysm flow diversion.²⁰

In this study, we present the FD-PComA IST, where we investigated the performance of the PED FD in PComA aneurysms with and without FPC. The FD-PComA IST demonstrated the application of computer modeling and simulation for generating evidence for less studied scenarios (FPC) and demographics (FPC prevalence varies across demographics). FD-PComA also targeted an off-label use of the PED FD and as such represents the largest scale study, clinical or otherwise, into PED treatment of PComA aneurysms.²³

METHODOLOGY

In-silico trial design

Hypotheses and subanalyses

In the FD-PComA IST, we hypothesized that: (i) maintained PComA flow following PED flow diversion of PComA aneurysms reduces treatment success (measured as postoperative aneurysm flow reduction) in patients with FPC; and (ii) PComA radius influences PComA aneurysm treatment success to a greater extent than aneurysm morphology, characterized by maximum diameter, aspect ratio, neck diameter, and non-sphericity index. In addition to flow reduction, endothelialization plays an important role in FD treatment²⁴ Therefore, we also investigate the influence of FPC on endothelialization,

Table 1 Flow diverter–posterior communicating artery (PComA) in-silico trial cohort characteristics for the 59 distinct anatomies included

Characteristics	
No of virtual patients	118
No of distinct geometries	59
Aneurysm location	
PComA (% (n/N))	100 (59/59)
Non-fetal posterior circulation (% (n/N))	50 (59/118)
Fetal posterior circulation (% (n/N))	50 (59/118)
Women (% (n/N))	74.6 (44/59)
Men (% (n/N))	25.4 (15/59)
Age (years) (mean±SD)	
Median (range)	53.0 (22.0–78.0)
Aneurysm size (mm) (mean±SD)	
Median (range)	5.0 (1.8–18.9)
Aneurysm neck (mm) (mean±SD)	
Median (range)	3.5 (1.6–8.8)
Aneurysm aspect ratio (mean±SD)	
Median (range)	1.3 (0.4–2.9)
Aneurysm non-sphericity index (mean±SD)	
Median (range)	0.17 (0.03–0.32)
PComA diameter (mm) (mean±SD)	
Median (range)	1.5 (0.5–2.2)
Demographic and morphological characteristics were identical in the non-fetal and fetal patients.	

using wall shear stress (WSS) on the device as a hemodynamic marker for endothelialization.^{25,26} Similar to flow reduction, we analyzed the influence of morphological parameters (PComA radius, aneurysm maximum diameter, aneurysm aspect ratio, aneurysm neck diameter, and aneurysm non-sphericity index) on endothelialization.

Inclusion criteria and virtual patient cohort

Patients were selected from the AneuX²⁷ and @neurIST cohorts.⁸ Inclusion criteria in the trial were that the patient must have only one aneurysm and that the aneurysm must arise from the PComA. In total, we selected 59 patients for the FD-PComA trial, with 13 anatomies from @neurIST and 46 from AneuX. We imposed distinct physiological flow conditions describing non-fetal and FPC in each anatomy, which gave us 59 virtual patients in each subgroup. Details of the cohort are shown in table 1.

Based on a retrospective study, the PED occlusion rate for PComA aneurysms is thought to be 43.7% for patients with FPC and 81.8% for patients without.⁶ Considering a type I error of 0.05 and a power of 90%, the number of subjects required to observe this disparity in treatment success in our trial was 64, with 32 from each subgroup (FPC and non-FPC).²⁸ The FD-PComA IST had 59 patients in each subgroup, which exceeded the number required to achieve statistical power in our results.

In-silico trial endpoints and other metrics

Clinical trials for FDs typically use endpoints such as neurological morbidity and mortality, intracranial hemorrhage, and ischemic stroke as measures of safety, and the angiographic occlusion rate at the 6 and 12 month follow-up as measures of efficacy. While it is not possible to simulate long term treatment

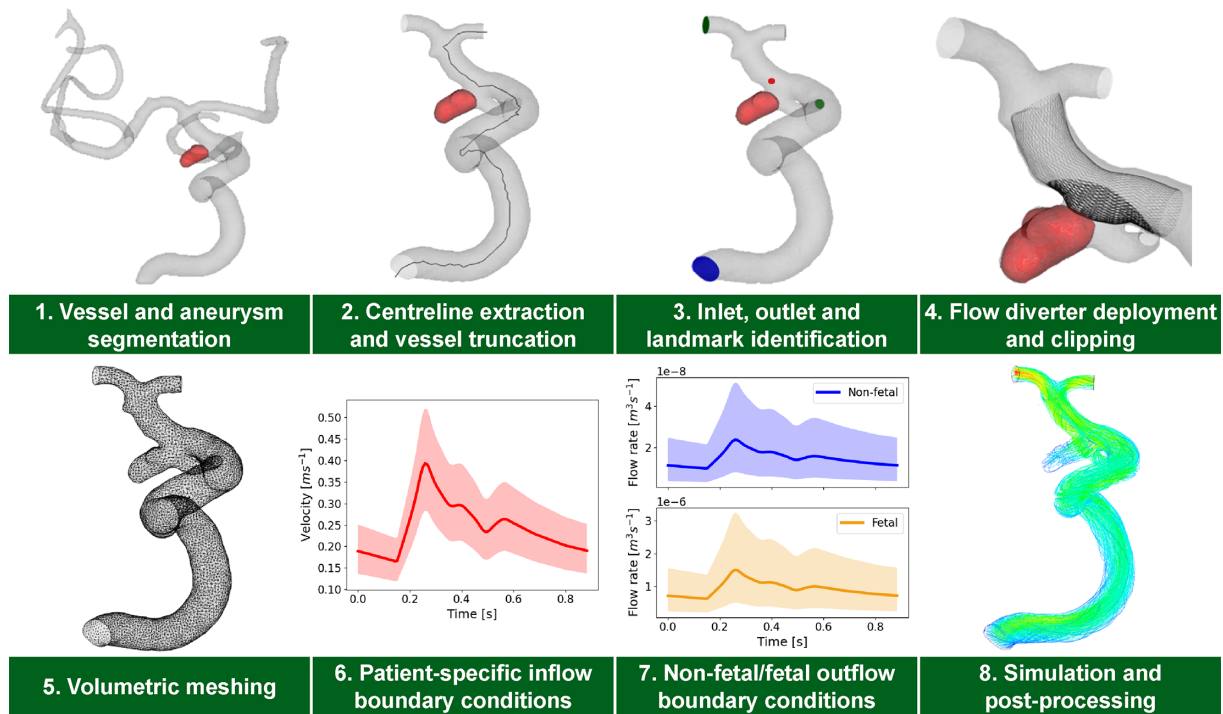


Figure 1 Flow diverter-posterior communicating artery in-silico trial simulation pipeline.

response currently, several studies suggest that post-treatment flow diversion is an appropriate proxy hemodynamic metric for predicting aneurysm occlusion.^{29 30} Furthermore, Sarrami-Foroushani *et al*²⁰ demonstrated that an in-silico endpoint of 35% reduction in aneurysm mean velocity led to accurate recreation of existing clinical trial results in a cohort of 82 internal carotid artery and PComA aneurysms. For this reason, we also considered a 35% reduction in aneurysm space and time-averaged velocity (STAV) as a hemodynamic surrogate endpoint for angiographic occlusion. As well as reducing the mean aneurysm velocity, FD treatment aims to reduce the maximum inflow velocity through the neck to minimize the impact of impinging jets.³¹ As such, reduction in maximum time-average velocity (MTAV) at the aneurysm neck has also been used as a hemodynamic proxy for successful occlusion.²⁰ We calculated this variable in addition to STAV and used it as another metric to assess aneurysm occlusion.

As well as stasis induced aneurysm thrombosis, endothelial cell growth along the device plays an important part in FD treatment of aneurysms.²⁴ WSS levels along the device struts have been shown to indicate the pattern of neointimal growth on the device.^{25 26} Increased WSS was found in regions that remained patent, whereas longitudinal proliferation of neointimal cells was found in regions of low WSS. Therefore, we used space and time-averaged WSS (STAWSS) on the device surface as an indicator of treatment performance. However, there are insufficient clinical or computational studies into this metric to formulate a suitable endpoint to distinguish successful or unsuccessful treatments.

In-silico trial simulation pipeline

The FD-PCoMA IST simulation pipeline is shown in [figure 1](#). Here, we provide an overview of the modeling steps shown in [figure 1](#). Each component of the pipeline is described in further detail in online supplemental material section 1.3.

Steps 1-3: for @neurIST patients, we segmented three-dimensional rotational angiography images to acquire segmented masks for the vessel and aneurysm.³² We then performed a series of additional pre-processing steps on the segmented masks, and on the surface meshes provided in the AneuX database, to acquire surface meshes for the internal carotid artery (ICA) inlet, the PComA outlet, the middle cerebral artery (MCA) outlet, the anterior cerebral artery (ACA) outlet, and the vessel (including the aneurysm).

Step 4: all patients were treated with a single PED FD in the FD-PCoMA IST. We positioned each FD in the ICA adjacent to the aneurysm neck and deployed the device using a fast virtual stent method.³³ To reduce computation costs, we clipped the FD, retaining the portion of the device covering the aneurysm neck and the branch PComA vessel.

Step 5: following surface mesh pre-processing and device deployment, volumetric meshes were generated for the pre-treatment and post-treatment configurations using ANSYS ICEM CFD V.19.1 (Ansys, Canonsburg, Pennsylvania, USA).

Steps 6 and 7: meshed anatomies were combined with virtual physiological flow conditions to create virtual patients. Flow conditions were applied through an inlet flow waveform generated using a multivariate gaussian model that takes the age and sex of a given virtual patient as its input.^{34 35} For each patient, we produced a waveform representing rest/normotensive conditions. To investigate our hypotheses, we developed outflow conditions that model the effect of non-fetal and fetal vascular physiology. Using data from Alastruey *et al*³⁶ and Zarrinkoob *et al*,¹³ we calculated flow split ratios between the ICA and PComA for patients with non-fetal and fetal circulation. We imposed these flow split conditions in our models as mass flow outlet boundary conditions on the PComA.

Step 8: blood flow simulations were performed by solving the unsteady Navier-Stokes equations in ANSYS CFX v19.1 (Ansys) using a finite volume method. Blood flow velocity from one cardiac cycle was extracted within the aneurysm sac and

the space-and-time-average of the velocity was used to calculate aneurysm STAV reduction as a percentage using $100\% \times (\text{STAV}_{pre} - \text{STAV}_{post})/\text{STAV}_{pre}$. To calculate MTAV, blood flow velocity was extracted in close proximity to the aneurysm neck surface. The time-average of the neck velocity was calculated and the maximum value of the time-averaged velocity was taken to be the 99th percentile. This value is referred to as MTAV and it was extracted pre-treatment and post-treatment to calculate aneurysm neck MTAV reduction similarly to STAV reduction. We extracted the WSS field on the FD surface in the post-treatment simulations and calculated STAWSS by taking the space-and-time-average of WSS across the entire clipped stent and all time steps.

RESULTS

Qualitative results

Visualizations of the velocity fields in non-fetal and fetal patients can help to develop an understanding of the impact that the different physiological conditions have on the aneurysm flow reduction. Figure 2 shows post-treatment systolic velocity streamlines for one patient under non-fetal and fetal flow conditions from two viewing angles. These visualizations demonstrate how the increased flow imposed through the PComA in the fetal patient draws a greater amount of blood flow across the FD and leads to higher residual flow in the aneurysm than in the non-fetal case. For this patient, the non-fetal aneurysm STAV reduction was 91.0%, whereas it was 62.1% in the fetal case. Given that all of the other factors were identical (eg, geometry, inflow conditions, and material properties), this highlights the large discrepancy in aneurysm flow reduction that is caused by non-fetal and fetal flow conditions. However, this result was only for one patient geometry and more significant results were found when analyzing the entire cohort.

Flow variables versus presence of fetal posterior circulation

Our three primary variables of interest were aneurysm STAV reduction, neck MTAV reduction, and stent STAWSS. We performed a t-test for each variable with the null hypothesis that the independent samples (non-fetal and fetal) had identical means assuming identical variances. We found that aneurysm STAV reduction was significantly lower in fetal cases than in non-fetal cases ($P < 10^{-3}$): mean STAV reduction was 67.8% in non-fetal patients but only 46.5% in fetal patients (figure 3, panel 1). We similarly found that aneurysm neck MTAV reduction was significantly lower in fetal than in non-fetal patients ($P = 10^{-3}$) (figure 3, panel 2). Flow reduction is a key feature of aneurysm treatment by flow diverting devices; these results correspondingly suggest that treatment success will be lower in patients with FPC. STAWSS on the device was also found to be significantly higher in fetal than in non-fetal patients ($P < 0.05$): mean STAWSS was 23.5 Pa in non-fetal patients and 29.2 Pa in fetal patients (figure 3, panel 3). Higher WSS suggests that endothelialization is more likely to be inhibited in patients with FPC.

Treatment success rate versus successful treatment threshold

Prediction of treatment success requires specification of threshold values for relevant variables of interest. In a previous in-silico study,²⁰ a 35% reduction in aneurysm STAV was used as a success criterion. With such a value, we found treatment success rates of 98.4% and 85.3% in non-fetal and fetal patients, respectively. These were substantially higher than the corresponding success rates (81.8% and 43.7%, respectively) reported by Rinaldo *et al.*⁶ Applying a 35% MTAV reduction threshold gave treatment

success rates of 63.9% and 32.8% in non-fetal and fetal patients, respectively. Figure 3 shows the predicted treatment success rates for a range of aneurysm STAV and MTAV threshold values, with the corresponding success rates from Rinaldo *et al.*⁶ These results suggest optimal matches between predicted success rates, and literature values were obtained with the following thresholds: STAV reduction of 50%, yielding non-fetal and fetal success rates of 88.5% and 42.6%, respectively; and MTAV reduction of 26%, yielding non-fetal and fetal success rates of 74.4% and 44.3%, respectively. These results demonstrate two key points: (i) there is a distinct difference in non-fetal versus fetal treatment success for a wide range of thresholds, and (ii) 35% STAV reduction is not applicable across different aneurysm subgroups or for different measures of flow reduction.

Flow variables versus morphological parameters

Statistical analyses were performed to test for correlation between flow variables and morphological parameters describing the aneurysm and the PComA. The flow variables tested were aneurysm STAV reduction, aneurysm neck MTAV reduction, and post-treatment stent STAWSS. Aneurysm morphology was characterized by maximum diameter, aspect ratio, neck width, and non-sphericity index. PComA size was characterized by its radius. The analyses were performed separately for the non-fetal and fetal subgroups. Linear regression was performed between each set of variables for each physiology. R^2 and P values are presented in online supplemental table 4 and plots of the results can be found in online supplemental material section 2.2. R^2 was low across all combinations, suggesting low correlation between flow variables and morphology in the non-fetal and fetal subgroups. P values were typically > 0.05 , demonstrating that best fit linear regression was not suitable for most variable combinations.

DISCUSSION

ISTs of ICA and PComA intracranial aneurysm flow diversion have been demonstrated to replicate and expand on results from conventional clinical trials.²⁰ In addition, each component of the FD-PComA IST modeling pipeline has been validated independently through a series of studies.^{8 32–35 37} Through the component-wise validations performed in these studies and the validation of the complete modeling pipeline performed by Sarrami-Foroushani *et al.*,²⁰ there is sufficient trust in the modeling choices to use the FD-PComA pipeline to investigate hypotheses for FD treatment indications that have not been studied in clinical trials and are not well understood.

The FD-PComA IST investigated PED FD treatment of PComA aneurysms in 118 virtual patients (59 geometries with non-fetal and FPC conditions imposed). In FPC patients, the PComA supplies the PCA and will typically be larger in diameter than in non-fetal patients. This highlights two factors that could reduce FD efficacy in PComA aneurysms in patients with FPC: the larger PComA diameter and the increased PComA flow rate. Our results demonstrated that an increased flow rate in FPC patients was associated with lower treatment success rates in terms of aneurysm STAV and MTAV reduction, which are hemodynamic markers of occlusion. Similarly, we found that patients with FPC had significantly higher STAWSS on the device struts than non-fetal patients, which has been linked to inhibited endothelialization and neointimal proliferation along the device struts.^{25 26} This will aid in maintaining PComA patency following treatment, which could explain why neurological complications following the treatment are rare.^{3–5}

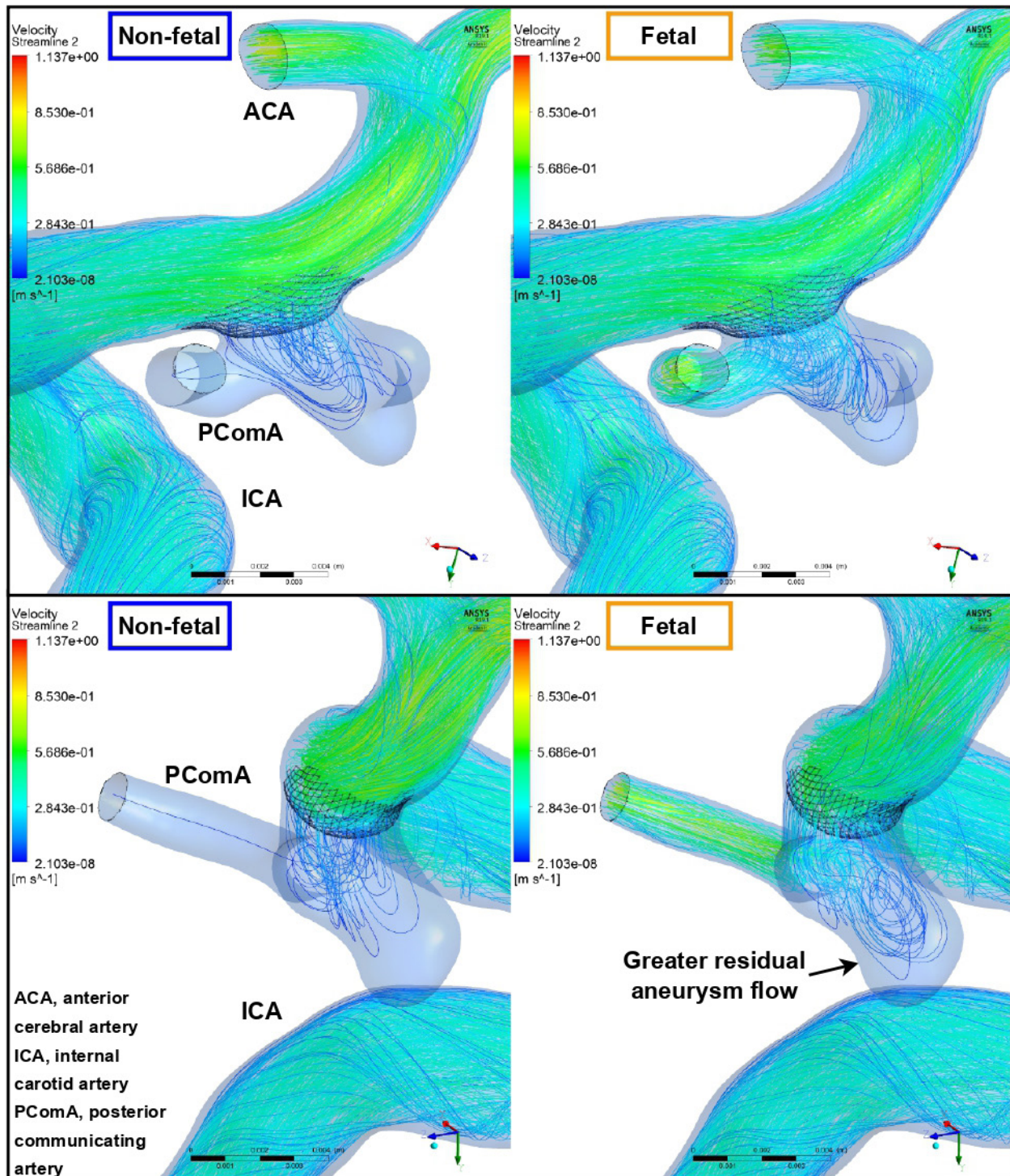
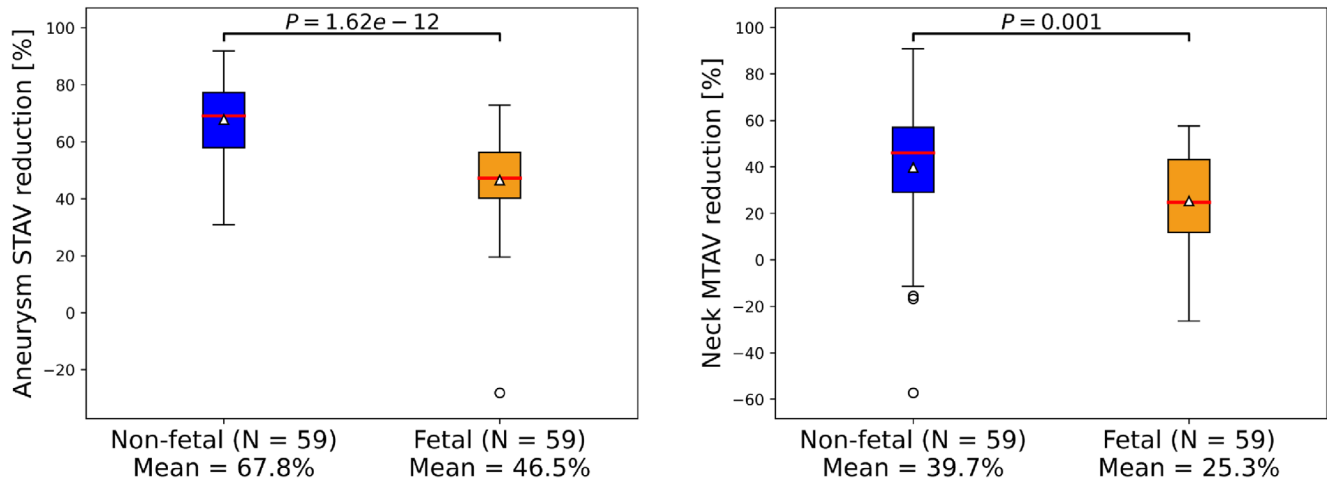


Figure 2 Systolic velocity streamlines for one patient from flow diverter–posterior communicating artery under non-fetal and fetal flow conditions. Aneurysm space-and-time-averaged velocity reduction was 91.0% for the non-fetal case and 62.1% for the fetal case. ACA, anterior cerebral artery; ICA, internal carotid artery; PComA, posterior communicating artery.

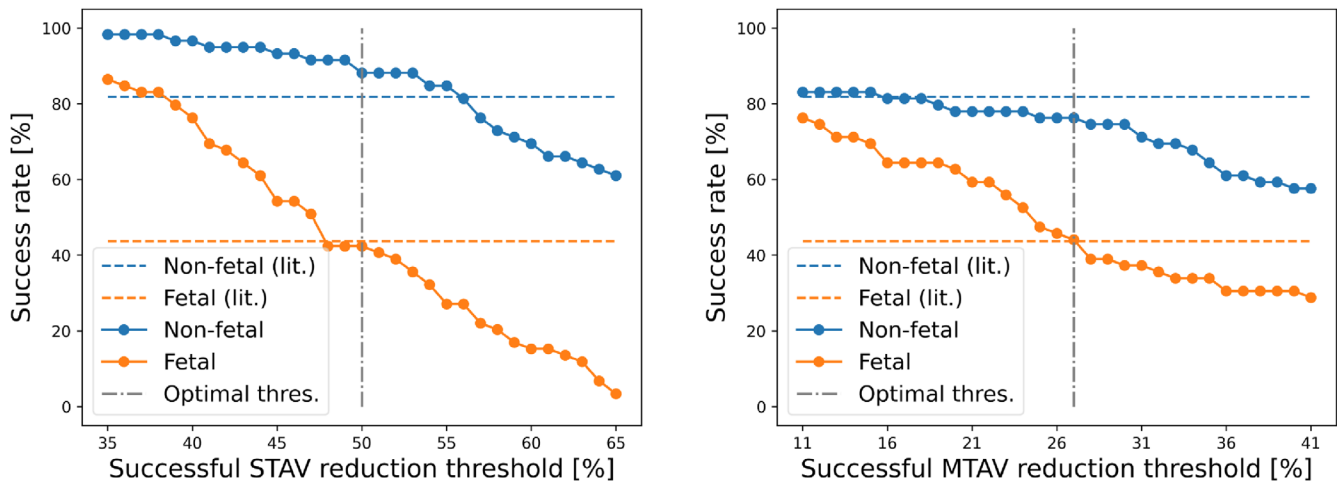
By construction, the PComA size distributions were identical in the non-fetal and fetal subgroups because the same anatomies were used in each. Aneurysm morphological characteristics (maximum diameter, aspect ratio, neck width, and non-sphericity index) were similarly identical across the non-fetal and fetal sub-groups. While this is a limitation of our IST (see further discussion in limitations), this allowed us to isolate the impact of physiology on treatment success. For this reason, it is clear that the difference in predicted treatment success is attributable

to the difference in flow rates in the subgroups rather than due to geometric differences. Despite the primary cause of reduced treatment efficacy being due to increased PComA flow rate, it is still possible to analyze the influence of PComA and aneurysm morphology within each subgroup. In doing this, P values <0.05 were found in the linear regression for the following combinations: non-fetal STAV reduction and aneurysm maximum diameter, non-fetal STAV reduction and aneurysm neck diameter, and fetal MTAV reduction and PComA radius. This suggests

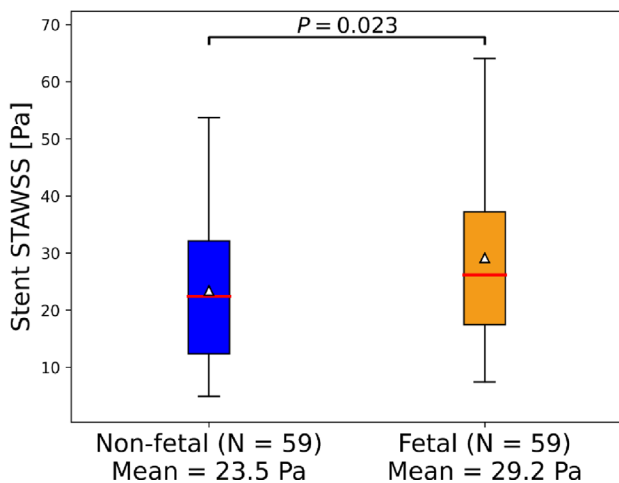
1. Flow reduction measures vs. non-fetal and fetal posterior circulation.



2. Non-fetal and fetal treatment success rates vs. flow reduction threshold defining success.



3. Stent wall shear stress vs. non-fetal and fetal posterior circulation.



Conclusions

1. Two measures of flow reduction are lower in patients with fetal posterior circulation, suggesting that aneurysm occlusion is less likely in fetal patients.
2. For a large range of flow reduction threshold values defining successful treatment, treatment success is lower in fetal than non-fetal patients.
3. Stent wall shear stress is greater in patients with fetal posterior circulation, suggesting hindered endothelialisation.

Figure 3 1 - Flow reduction characterised by aneurysm STAV and MTAV reduction plotted. For nonfetal and fetal physiology. 2 - Treatment success rates against different STAV/MTAV reduction thresholds. 3 - Stent WSS plotted against non-fetal and fetal physiology. MTAV, maximum timeaveraged velocity; STAV, space-and-time-averaged velocity; WSS, wall shear stress.

that despite the P values being typically >0.05 , the aneurysm morphology had a slightly stronger influence on flow reduction in the non-fetal subgroup than in the fetal group.

Our results indicate that fetal PComA aneurysms treated by PED flow diversion will have low aneurysm flow reduction due to the persistent flow through the PComA. This could explain the slow or failed occlusion that is observed more predominantly in patients with FPC than in those without.⁶ Endovascular coiling is more straightforward in PComA aneurysms than in other anterior circulation aneurysms due to the relative ease of access.¹ Therefore, in patients with FPC, using endovascular coils in conjunction with flow diversion may be a viable option to improve aneurysm flow reduction and accelerate occlusion. Stent assisted coiling has already been shown to be effective in treating PComA aneurysms, but further studies are required to ascertain the efficacy of FD assisted coiling.³⁸

FPC is estimated to occur in 4–29% of the population,¹ but its prevalence can vary across different demographics. Shaban *et al*¹⁰ retrospectively reviewed 532 PComA aneurysms and provided statistics for the prevalence of FPC in a number of races. We collated these data (see online supplemental table 1) and found that full FPC prevalence was significantly lower in white (4.9%, 8/164) than in black patients (11.5%, 40/349, $P=0.008$). The FD-PComA IST therefore not only generated evidence in less studied scenarios (PComA aneurysms with FPC), but also provided insights that could be beneficial to demographic groups that are sometimes under-represented in clinical trials (black race).³⁹ Conducting ISTs to generate medical device safety and efficacy evidence for demographics and subgroups that were previously less studied in clinical trials highlights how ISTs can be used to improve health equity.

Limitations

FD-PComA did not explicitly include patient race in the models in a way that allowed for this aspect of the cohort demographic to be controlled. Instead, we developed boundary conditions that described FPC in the knowledge that fetal boundary conditions model a phenomena that is more common in patients of black race due to their higher FPC prevalence. This limitation could be overcome by using a dataset that includes racial information for an array of PComA aneurysms and then defining suitable inclusion/exclusion criteria to design a trial cohort that includes the desired subgroups, but such a data set was not available.

Angiography images encompassing the entire brain vasculature were similarly unavailable for our study, precluding the direct identification of fetal and non-fetal patients based on anatomical configurations. Consequently, we adopted a methodology where we simulated fetal and non-fetal physiological conditions for each anatomical model by applying flow rate values obtained from existing literature. It is important to acknowledge that this approach assumes independence between vascular anatomy and physiology, a consideration to bear in mind when interpreting our findings. It is similarly important to note that while our non-fetal and fetal flow splits were checked to fall within the expected bounds based on clinical literature, we did not perform direct validation of our simulation results with clinical data. Nonetheless, the approach we took facilitated a comparative analysis of treatment efficacy under distinct physiological conditions within identical anatomical cohorts. Such control over sources of variability is often lacking in traditional clinical trials, underscoring the value of in-silico in minimizing confounding factors.

Biological processes such as stasis/device driven thrombosis and PComA remodeling were not modeled. Stasis driven thrombosis plays an important part in aneurysm treatment success

and clot composition has been linked to ischemic/hemorrhagic stroke.^{31 40} Device-induced thrombosis is an alternative clotting pathway that links to endothelial cell growth along the device, which is another component of successful FD treatment.²⁴ PComA remodeling can occur as a long term result of FD treatment affecting the PComA flow rate and the vessel subsequently adapting to the increased/decreased flow. Modeling stasis/device-induced thrombosis would require coupling biochemical models to the blood flow model, such as in Sarrami-Foroushani *et al*,³⁷ but this was not deemed necessary to address the FD-PComA trial hypotheses. In FD-PComA, we assumed that PComA flow rates were the same before and after treatment to address the hypotheses regarding FPC, which meant that investigating remodeling was not feasible. Addressing these limitations could form the basis for additional ISTs.

CONCLUSIONS

The FD-PComA IST provided evidence suggesting that (1) PED FD treatment of PComA aneurysms is less effective in patients with FPC and (2) this is due to the increased flow rate through the PComA in this scenario. We found that morphological variables such as PComA size, aneurysm maximum diameter, aneurysm aspect ratio, aneurysm neck width, and aneurysm non-sphericity index did not influence the treatment outcome as strongly as flow rate through the PComA. Relating our findings to the trial hypotheses, we conclude that: (i) maintained PComA flow following flow diversion reduces treatment success rates in patients with FPC, and (ii) PComA aneurysm FD treatment success is most affected by the presence of FPC and was not significantly influenced by PComA diameter, aneurysm maximum diameter, aspect ratio, neck width, or the non-sphericity index. Endothelialization, as characterized by WSS on the device surface, was also hindered by the presence of FPC and not influenced by the morphology of the PComA or aneurysm. Given these findings, we suggest that PComA aneurysm patients with FPC should be treated with an alternative to single PED FD treatment.

X Alejandro F Frangi @affrangi

Contributors MM: conceptualization, investigation, methodology, software, formal analysis, writing-original draft, writing-review, and editing. AS-F: conceptualization, investigation, methodology, software, supervision, writing-review, and editing. SS: methodology and software. QL: methodology and software. CK: software. NR: software. TP: conceptualization, TL: conceptualization, supervision, writing-review, and editing. ZAT: conceptualization, supervision, writing-review, and editing. AFF: conceptualization, funding acquisition, supervision, writing-review and editing. AFF is the guarantor. The AI technology used is called deep learning, which we used for medical image analysis. Specifically, we used convolutional neural networks to perform segmentation. Segmentation is used to reconstruct vascular surface meshes from 3D rotational angiography images. The vascular surface meshes were manually checked by eye to ensure realistic results for every patient. The method we used is published in Lin *et al*.³²

Funding AFF acknowledges support from the Royal Academy of Engineering under the RAEng Chair in Emerging Technologies (INSILEX CIET1919/19) and ERC Advanced Grant—UKRI Frontier Research Guarantee (INSILICO EP/Y030494/1) schemes. AFF acknowledges seminal funding from the European Commission to @neurIST (FP6-2004-IST-4-027703) and the @neurIST Consortium. AS-F, TL, and AFF were funded by the European Commission via InSilc (H2020-SC1-2017-CNECT-2-777119). ZAT was funded by a Royal Academy of Engineering/Leverhulme Trust Research Fellowship (No LTRF2021/17115). MM was supported by the Engineering and Physical Sciences Research Council (EPSRC) Centre for Doctoral Training in Fluid Dynamics (P/L01615X/1). We acknowledge support from ANSYS through an Academic Partnership Agreement (No 1122349). The information contained herein reflects only the authors' view, and none of the funders or the European Commission are responsible for any use that may be made of it.

Competing interests None declared.

Patient consent for publication Not applicable.

Ethics approval Not applicable.

Provenance and peer review Not commissioned; externally peer reviewed.

Data availability statement Data are available upon reasonable request. The data that support the findings of this study are available from the corresponding author upon reasonable request as part of a collaborative research project.

Supplemental material This content has been supplied by the author(s). It has not been vetted by BMJ Publishing Group Limited (BMJ) and may not have been peer-reviewed. Any opinions or recommendations discussed are solely those of the author(s) and are not endorsed by BMJ. BMJ disclaims all liability and responsibility arising from any reliance placed on the content. Where the content includes any translated material, BMJ does not warrant the accuracy and reliability of the translations (including but not limited to local regulations, clinical guidelines, terminology, drug names and drug dosages), and is not responsible for any error and/or omissions arising from translation and adaptation or otherwise.

Open access This is an open access article distributed in accordance with the Creative Commons Attribution Non Commercial (CC BY-NC 4.0) license, which permits others to distribute, remix, adapt, build upon this work non-commercially, and license their derivative works on different terms, provided the original work is properly cited, appropriate credit is given, any changes made indicated, and the use is non-commercial. See: <http://creativecommons.org/licenses/by-nc/4.0/>.

ORCID iDs

Michael MacRaid <http://orcid.org/0009-0001-3307-743X>

Qiongyao Liu <http://orcid.org/0000-0001-8534-8791>

Zeike A Taylor <http://orcid.org/0000-0002-0718-1663>

Alejandro F Frangi <http://orcid.org/0000-0002-2675-528X>

REFERENCES

- Golshani K, Ferrell A, Zomorodi A, *et al.* A review of the management of posterior communicating artery aneurysms in the modern era. *Surg Neurol Int* 2010;1:88.
- US FDA. General issues: meeting to discuss the evaluation of safety and effectiveness of endovascular medical devices intended to treat intracranial aneurysms. Technical report, US Food and Drug Administration; 2018. Available: <https://www.fda.gov/media/111329/download>
- Daou B, Valle-Giler EP, Chalouhi N, *et al.* Patency of the posterior communicating artery following treatment with the Pipeline Embolization Device. *J Neurosurg* 2017;126:564–9.
- Kühn AL, Dabus G, Kan P, *et al.* Flow-diverter stents for endovascular management of non-fetal posterior communicating artery aneurysms—analysis on aneurysm occlusion, vessel patency, and patient outcome. *Interv Neuroradiol* 2018;24:363–74.
- Enriquez-Marulanda A, Ravindran K, Salem MM, *et al.* Evaluation of Radiological Features of the Posterior Communicating Artery and Their Impact on Efficacy of Saccular Aneurysm Treatment with the Pipeline Embolization Device: A Case Series Study. *World Neurosurg* 2019;125:e998–1007.
- Rinaldo L, Brinjikji W, Cloft H, *et al.* Effect of Fetal Posterior Circulation on Efficacy of Flow Diversion for Treatment of Posterior Communicating Artery Aneurysms: A Multi-Institutional Study. *World Neurosurg* 2019;127:e1232–6.
- van Raamt AF, Mali WPTM, van Laar PJ, *et al.* The fetal variant of the circle of Willis and its influence on the cerebral collateral circulation. *Cerebrovasc Dis* 2006;22:217–24.
- Villa-Urriol MC, Berti G, Hose DR, *et al.* @neurIST complex information processing toolchain for the integrated management of cerebral aneurysms. *Interface Focus* 2011;1:308–19.
- Thiarawat P, Jahromi BR, Kozyrev DA, *et al.* Are Fetal-Type Posterior Cerebral Arteries Associated With an Increased Risk of Posterior Communicating Artery Aneurysms? *Neurosurg* 2019;84:1306–12.
- Shaban A, Albright KC, Boehme AK, *et al.* Circle of Willis Variants: Fetal PCA. *Stroke Res Treat* 2013;2013:105937.
- Zanaty M, Chalouhi N, Starke RM, *et al.* Failure of the Pipeline Embolization Device in Posterior Communicating Artery Aneurysms Associated with a Fetal Posterior Cerebral Artery. *Case Rep Vasc Med* 2016;2016:1–4.
- Wallace AN, Kayan Y, Austin MJ, *et al.* Pipeline embolization of posterior communicating artery aneurysms associated with a fetal origin posterior cerebral artery. *Clin Neurol Neurosurg* 2017;160:83–7.
- Zarrinkoob L, Ambarki K, Wählin A, *et al.* Blood Flow Distribution in Cerebral Arteries. *J Cereb Blood Flow Metab* 2015;35:648–54.
- Becske T, Kallmes DF, Saatci I, *et al.* Pipeline for uncoilable or failed aneurysms: results from a multicenter clinical trial. *Radiology* 2013;267:858–68.
- Hanel RA, Kallmes DF, Lopes DK, *et al.* Prospective study on embolization of intracranial aneurysms with the pipeline device: the PREMIER study 1 year results. *J NeuroIntervent Surg* 2020;12:62–6.
- Kallmes DF, Brinjikji W, Boccardi E, *et al.* Aneurysm Study of Pipeline in an Observational Registry (ASPIRe). *Intervent Neurol* 2016;5:89–99.
- Kallmes DF, Hanel R, Lopes D, *et al.* International Retrospective Study of the Pipeline Embolization Device: A Multicenter Aneurysm Treatment Study. *Am J Neuroradiol* 2015;36:108–15.
- Buffenstein I, Kaneakua B, Taylor E, *et al.* Demographic recruitment bias of adults in United States randomized clinical trials by disease categories between 2008 to 2019: a systematic review and meta-analysis. *Sci Rep* 2023;13:42.
- Pappalardo F, Russo G, Tshinanu FM, *et al.* In silico clinical trials: concepts and early adoptions. *Brief Bioinformatics* 2019;20:1699–708.
- Sarrami-Foroushani A, Lassila T, MacRaid M, *et al.* In-silico trial of intracranial flow diverters replicates and expands insights from conventional clinical trials. *Nat Commun* 2021;12:3861.
- Miller C, Padmos RM, van der Kolk M, *et al.* In silico trials for treatment of acute ischemic stroke: Design and implementation. *Comput Biol Med* 2021;137:104802.
- Adegbola PI, Fadahunsi OS, Adegbola AE, *et al.* In silico studies of potency and safety assessment of selected trial drugs for the treatment of COVID-19. *In Silico Pharmacol* 2021;9:45.
- Patel PD, Chalouhi N, Atallah E, *et al.* Off-label uses of the Pipeline embolization device: a review of the literature. *Neurosurg Focus* 2017;42:E4.
- Ravindran K, Salem MM, Alturki AY, *et al.* Endothelialization following Flow Diversion for Intracranial Aneurysms: A Systematic Review. *AJNR Am J Neuroradiol* 2019;40:295–301.
- Berg P, Iosif C, Ponsonnard S, *et al.* Endothelialization of over- and undersized flow-diverter stents at covered vessel side branches: An in vivo and in silico study. *J Biomech* 2016;49:4–12.
- Benard N, Coisne D, Donal E, *et al.* Experimental study of laminar blood flow through an artery treated by a stent implantation: characterisation of intra-stent wall shear stress. *J Biomech* 2003;36:991–8.
- Juchler N, Schilling S, Bijlenga P, *et al.* Shape Trumps Size: Image-Based Morphological Analysis Reveals That the 3D Shape Discriminates Intracranial Aneurysm Disease Status Better Than Aneurysm Size. *Front Neurol* 2022;13:809391.
- Schmidt SAJ, Lo S, Hollestein LM. Research Techniques Made Simple: Sample Size Estimation and Power Calculation. *J Invest Dermatol* 2018;138:1678–82.
- Uared R, Larrabide I, Brina O, *et al.* Computational fluid dynamics analysis of flow reduction induced by flow-diverting stents in intracranial aneurysms: a patient-unspecific hemodynamics change perspective. *J NeuroIntervent Surg* 2016;8:1288–93.
- Mut F, Raschi M, Scrivano E, *et al.* Association between hemodynamic conditions and occlusion times after flow diversion in cerebral aneurysms. *J NeuroIntervent Surg* 2015;7:286–90.
- Kulcsár Z, Houdart E, Bonafé A, *et al.* Intra-Aneurysmal Thrombosis as a Possible Cause of Delayed Aneurysm Rupture after Flow-Diversion Treatment. *AJNR Am J Neuroradiol* 2011;32:20–5.
- Lin F, Xia Y, Song S, *et al.* High-throughput 3DRA segmentation of brain vasculature and aneurysms using deep learning. *Comput Methods Programs Biomed* 2023;230:107355.
- Larrabide I, Kim M, Augsburger L, *et al.* Fast virtual deployment of self-expandable stents: Method and in vitro evaluation for intracranial aneurysmal stenting. *Med Image Anal* 2012;16:721–30.
- Lassila T, Sarrami-Foroushani A, Hejazi S, *et al.* Population-specific modelling of between/within-subject flow variability in the carotid arteries of the elderly. *Int J Numer Method Biomed Eng* 2020;36:e3271.
- Sarrami-Foroushani A, Lassila T, Gooya A, *et al.* Uncertainty quantification of wall shear stress in intracranial aneurysms using a data-driven statistical model of systemic blood flow variability. *J Biomech* 2016;49:3815–23.
- Alastruey J, Parker KH, Peiró J, *et al.* Modelling the circle of Willis to assess the effects of anatomical variations and occlusions on cerebral flows. *J Biomech* 2007;40:1794–805.
- Sarrami-Foroushani A, Lassila T, Hejazi SM, *et al.* A computational model for prediction of clot platelet content in flow-diverted intracranial aneurysms. *J Biomech* 2019;91:7–13.
- Cho YD, Lee WJ, Kim KM, *et al.* Stent-assisted coil embolization of posterior communicating artery aneurysms. *AJNR Am J Neuroradiol* 2013;34:2171–6.
- Turner BE, Steinberg JR, Weeks BT, *et al.* Race/ethnicity reporting and representation in US clinical trials: A cohort study. *Lancet Reg Health Am* 2022;11:100252.
- Brinjikji W, Lanzino G, Cloft HJ, *et al.* Risk Factors for Ischemic Complications following Pipeline Embolization Device Treatment of Intracranial Aneurysms: Results from the IntrePED Study. *AJNR Am J Neuroradiol* 2016;37:1673–8.

Supplementary Material

Off-label in-silico flow diverter performance assessment in posterior communicating artery aneurysms

Michael MacRaidl^{1,2,5*}, Ali Sarrami-Foroushani^{1,6}, Shuang Song³, Qiongyao Liu³, Christopher Kelly³, Nishant Ravikumar^{1,3}, Tufail Patankar⁹, Toni Lassila³, Zeike A. Taylor⁴, and Alejandro F. Frangi^{1,5,6,7,8*}

¹Centre for Computational Imaging and Modelling in Medicine (CIMIM), University of Manchester, Manchester, UK

²EPSRC Centre for Doctoral Training in Fluid Dynamics, University of Leeds, Leeds, UK.

³School of Computing, University of Leeds, Leeds, UK.

⁴School of Mechanical Engineering, University of Leeds, Leeds, UK.

⁵Department of Computer Science, School of Engineering, University of Manchester, Manchester, UK.

⁶School of Health Sciences, Division of Informatics, Imaging and Data Sciences, University of Manchester, Manchester, UK.

⁷Department of Cardiovascular Sciences, KU Leuven, Leuven, Belgium.

⁸Department of Electrical Engineering (ESAT), KU Leuven, Leuven, Belgium.

⁹Leeds General Infirmary, Leeds, UK

*Corresponding authors: Michael MacRaidl; Alejandro F. Frangi

e-mail: michael.macraidl@manchester.ac.uk;

alejandro.frangi@manchester.ac.uk

Mailing address: The University of Manchester, Oxford Road, Manchester, M13 9PL

1 Methodology

1.1 Fetal posterior circulation

Figure 1 shows images of fetal and non-fetal patients from the @neurIST database. In the fetal case, the PComA is larger and supplying blood to the posterior circulation. In the non-fetal case, the PComA is less visible in the image. This is due to less contrast agent being drawn into the PComA as it supplies no distal vessels and therefore has a reduced flow rate. These images highlight the two factors that could reduce flow diverter efficacy in PComA aneurysms in patients with FPC: the increased flow rate and the increased PComA size.

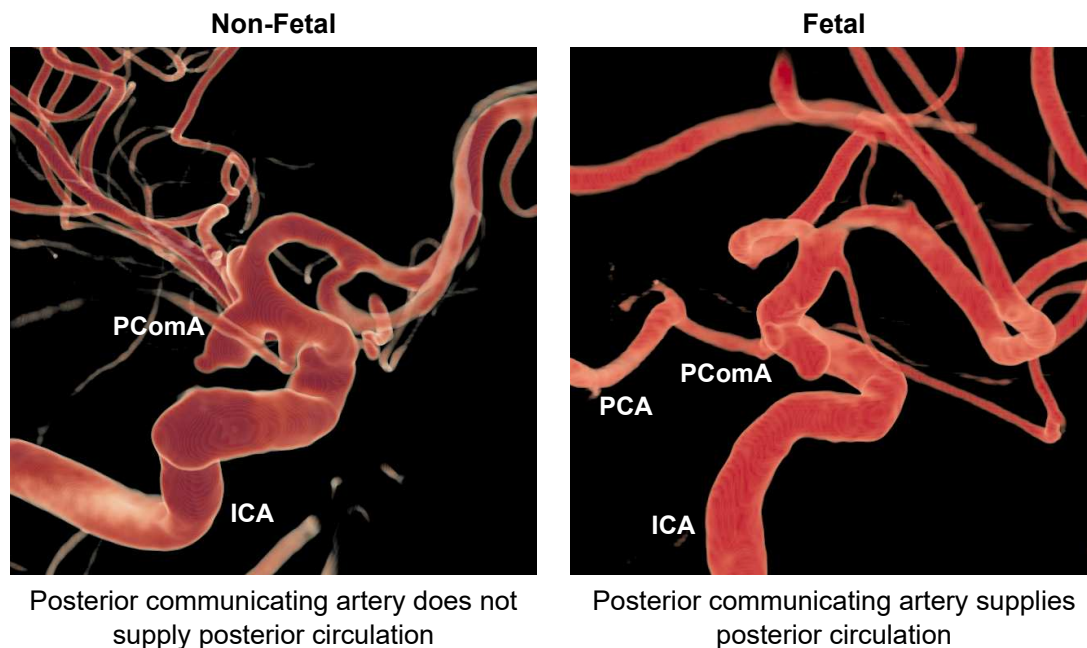


Figure 1: Non-fetal and fetal vasculature for patient cases from the @neurIST database. In the non-fetal image, the PComA is thin and has little flow through it. In the fetal image, the PComA is larger and supplies the distal PCA. ICA, internal carotid artery; PComA, posterior communicating artery; PCA, posterior cerebral artery.

Table 1: Fetal posterior circulation prevalence for different races.

Reference	FPC Classification	Race		
		White	Black	Hispanic
Shaban et al. [1]	Fetal, % (<i>n/N</i>)	4.9 (8/164)	11.5 (40/349)	0 (0/12)
	Partial fetal, % (<i>n/N</i>)	15.2 (25/164)	14.9 (52/349)	16.7 (2/12)
	Fetal or partial fetal, (<i>n/N</i>)	20.1 (33/164)	26.4 (92/349)	16.7 (2/12)
	Non-fetal, % (<i>n/N</i>)	79.9 (131/164)	73.6 (257/349)	83.3 (10/12)

FPC, fetal posterior circulation.

1.2 In-silico trial design

Hypotheses and sub-analyses See details in main manuscript.

Power calculation See details in main manuscript.

Inclusion criteria and virtual patient cohort We initially processed a number of cases directly from @neurIST images. The @neurIST cohort consists of 3D rotational angiography images for 800 patients, 143 of which are for PComA aneurysms. We selected 27 of these images and automatically segmented them using an algorithm developed by Lin et al. [2]. Following segmentation and subsequent surface mesh processing and device deployment steps, 13/27 patients were added to the trial. The AneuX cohort contains surface meshes for 668 vessels and

750 aneurysm domes gathered by processing patients from the AneuX1, AneuX2, @neurIST and Aneurisk data sets. We randomly selected 60 of the 130 PComA cases in AneuX, ensuring no duplication with the successful @neurIST cases, eventually retaining 46/60 cases. In total, we had 59 in the FD-PComA trial, with 13 anatomies from @neurIST and 46 from AneuX.

In-silico trial end points and other metrics See details in main manuscript.

1.3 In-silico trial simulation pipeline

Image segmentation (Manuscript Figure 1 panel 1) The @neurIST database contains 3D rotational angiography images for each patient. These images were automatically segmented using a multi-task convolutional neural network and a patch-based learning pipeline designed to segment both vessel and aneurysm simultaneously [2]. In the AneuX database, surface meshes for vessel and aneurysm are provided and segmentation was not necessary.

Surface mesh pre-processing (Manuscript Figure 1 panels 2 and 3) Following automatic segmentation of the 3DRA images, we processed the segmented masks to prepare vascular surface meshes for subsequent volume meshing. First, centrelines were extracted using CGAL mesh skeletonisation [3]. This process includes mean flow curvature computation, skeleton contraction and extraction and post-processing on the extracted skeleton (e.g. smoothing, optimisation) to ensure the resulting centreline is accurate and high quality. The centreline points were used to identify bifurcation and terminal locations in the vasculature. We used the segmented aneurysm mask (@neurIST) or sac mesh (AneuX) to identify an aneurysm landmark point on the centreline, which was later used to position the flow diverter during device deployment. Bifurcation and terminal centreline points were used to identify the ICA-PComA bifurcation, the middle/anterior cerebral artery (MCA-ACA) bifurcation, the ICA inlet, and the PComA, MCA and ACA outlets. Manual surface corrections were applied where required, particularly to remove small vessels for which we did not have appropriate boundary conditions, such as the anterior choroidal artery. The PComA, MCA and ACA were clipped or extruded as required to ensure that they had a comparable length while retaining as much of the PComA as possible. These steps produced surface meshes for the inlet (ICA), three outlets (PComA, MCA, ACA), and vessel (including the aneurysm).

Flow diverter deployment (Manuscript Figure 1 panel 4) All patients were treated with a single PED flow diverter. Each PED consisted of 48 wires with a 30 μm thickness and was deployed using a fast virtual stent (FVS) placement method, which was presented and validated by Larrabide et al. [4]. We positioned each flow diverter using the aneurysm location landmark and selected flow diverter diameter using the mean of the parent vessel radii proximal and distal to the aneurysm landmark. To reduce computation costs, we clipped the flow diverter, which has been shown to have negligible effect on intra-aneurysmal haemodynamics [5]. When clipping, we retained the portion of the flow diverter covering the aneurysm neck and the branch PComA vessel.

Volumetric meshing (Manuscript Figure 1 panel 5) Following surface mesh pre-processing and device deployment, volumetric meshes were generated using ANSYS ICEM CFD v19.1 (Ansys Inc., Canonsburg, PA, USA). Tetrahedral elements with maximum edge size of 0.5 mm were used to discretise the computational domain. A maximum edge size of 0.2 mm was used on the vessel wall and 0.05 mm was used on the inlet and outlet surfaces. Where PED was present, a

maximum edge size of 0.01 mm was set on the wires. This led to an average number of mesh elements across all geometries of approximately 1 million without device and 14 million with. Mesh independence of the solutions at these resolutions was verified by Sarrami-Foroushani et al. [6].

Inflow boundary conditions (Manuscript Figure 1 panel 6) Normotensive ICA flow waveforms were taken as the mean of the MGM, which was trained and calibrated by patient-specific phase-contrast magnetic resonance imaging measurements of ICA flow in 17 healthy young adults (age = 28 ± 7 years) [7].

Non-fetal and fetal outflow boundary conditions (Manuscript Figure 1 panel 7) To investigate our hypotheses, we developed outflow conditions that model the effect of non-fetal and fetal vascular physiology. Alastruey et al. [8] developed a 1D model of the Circle of Willis and calculated flow rates in the large vessels after removing various vascular segments from the model. Using data from this paper (see Supplementary Table 2), we calculated the mean volume flow rate in the ICA by summing the flow rates of the ACA, MCA and PComA for a given side of the vasculature (i.e. left or right). We used the ratio of ICA inflow to PComA outflow to calculate a ratio of PComA to ICA flow for non-fetal and fetal cases. The fetal/non-fetal flow splits are multiplied by the ICA inflow derived from the MGM to calculate outflow rates for the PComA in fetal and non-fetal conditions. For non-fetal and fetal patients, we multiplied the inflow rates by 0.34% and 21.7% to get the PComA outflow rates, respectively. We used the flow splits to calculate mass flow rates for non-fetal and fetal cases and imposed them as mass flow outlet boundary conditions on the PComA. This allowed us to model distinct physiological conditions for each geometry.

Alastruey et al. [8] developed their 1D model based on one set of vessel parameters. To check that the derived flow splits fall within the expected variability across a range of patients, we also analysed data from a clinical study [9]. Zarrinkoob et al. [9] used phase-contrast MRI to assess cerebral blood flow (CBF) in 94 patients, 17 of which were fetal. In their results, they found that the percentage of total CBF (tCBF) in the P1 PCA was unchanged for fetal vs. non-fetal patients ($8 \pm 1\%$). For fetal patients this blood can only be supplied by the PComA, so we deduce that the PComA also accounts for $8 \pm 1\%$ of the tCBF. In fetal patients, the ipsilateral ICA accounts for $40 \pm 3\%$ of the tCBF. The PComA therefore accounts for $20 \pm 3\%$ of the ICA flow. From Zarrinkoob et al. [9], we can also calculate the PComA flow ratio in non-fetal patients to be $2.6 \pm 2.3\%$ (see Appendix Table 2). The flow splits from Alastruey et al. [8] fall within the confidence intervals of the flow splits from Zarrinkoob et al. [9] for the fetal and right-sided non-fetal cases. As the left side non-fetal flow split (-0.35%) from Alastruey et al. [8] was outside the bounds of the flow split calculated from Zarrinkoob et al. [9], we did not consider this scenario.

Table 2: Flow-rate split ratios for non-fetal and fetal posterior circulation patients. Table A: Mean volume flow-rates (ml/s) at the outlet of the efferent arteries and in the middle of the communicating arteries for different study cases from [8]. Complete circle is non-fetal and RPCA/LPCA absent is fetal. ICA flow is calculated as the sum of ACA, MCA and PComA outflow. Table B: Mean percentage of total cerebral blood flow measured in each artery “All” patients ($N = 94$) and “Fetal” ($N = 17$) patients in each vessel with standard deviations from [9]. “Non-fetal” mean values are calculated using $\mu_{nf} = (\mu_{all}N_{all} - \mu_f N_f)/(N_{all} - N_f)$ and standard deviations are taken as the standard deviation of “All”. The “PComA” column values for “All” and “Non-fetal” are the remaining ICA flow percentage once the percentages for OA, MCA and ACA are subtracted. For “Fetal”, the PComA flow percentage is simply the PCA flow percentage, as the PComA is the only supplier of the PCA. PComA to ICA flow ratios and standard deviations are calculated from the PComA and ICA mean flow percentages and standard deviations.

Table A: Alastruey et al. [8]

Study case	Side	ACA	MCA	PComA	PComA:ICA [%]
Complete circle	Right	1.16	1.73	-0.01	0.34
Complete circle	Left	1.16	1.72	0.01	-0.35
PCA (P1) absent	Right	1.15	1.70	-0.79	21.7
PCA (P1) absent	Left	1.15	1.70	-0.79	21.7

Table B: Zarrinkoob et al. [9]

Study case	ICA	OA	ACA	MCA	PCA	BA	PComA	PComA:ICA [%]
All ($N = 94$)	36±4	2±1	11±4	21±3	8±1	20±4	2±1	5.6 ±3
Fetal ($N = 17$)	40±3	2±1	10±2	21±3	8±1	15±4	8±1	20±3
Non-fetal ($N = 77$)	35.1±4	2±1	11.2±4	21±3	8±1	21.1±4	0.9±1	2.6±2.3

ACA, anterior cerebral artery; BA, basilar artery; ICA, internal carotid artery; LPCA, left PCA; MCA, middle cerebral artery; OA, ophthalmic artery; PCA, posterior cerebral artery; PComA, posterior communicating artery; RPCA, right PCA.

Computational fluid dynamics simulations (Manuscript Figure 1 panel 8) Arterial wall distensibility was not considered and blood was modelled as an incompressible, Newtonian fluid with density 1066 kgm^{-3} and dynamic viscosity of 0.0035 Pa.s . The cardiac cycle was discretised into 200 equal steps; timestep independence studies were performed previously by Villa-Uriol et al. [10], Cebral et al. [11]. Each simulation was run for three cardiac cycles and results from the last cycle were analysed to reduce the effect of initial transients. No-slip boundary conditions were applied on vessel walls and zero pressure was applied at the ACA and MCA outlets see further details of this in Supplementary Section 2.1). ICA Inflow and PComA outflow conditions were as described previously.

Post-processing and analysis (Manuscript Figure 1 panel 8) The aneurysm and vessel geometries were not separated for in the simulation models, but the aneurysm sac mesh was used to post-process the aneurysm flow quantities. For the AneuX data, the aneurysm sac meshes were provided. For the @neurIST data, we manually clipped the neck surface using Paraview [12] and used this to extract the aneurysm sac mesh. In both data sets, the aneurysm neck was defined as a plane that cuts the aneurysm only (i.e. the neck surface did not clip the aneurysm and PComA, but only the aneurysm sac). This neck surface choice is referred to as the “dome” cut in Juchler et al. [13].

Once the aneurysm sac was identified, aneurysm velocity was extracted on the mesh nodes within the aneurysm sac and interpolated onto a linearly spaced 3D grid. The space-and-time-

average of the interpolated velocity was calculated pre- and post-treatment and used to calculate aneurysm STAV reduction as a percentage using $100\% \times (\text{STAV}_{pre} - \text{STAV}_{post})/\text{STAV}_{pre}$. To calculate MTAV, velocity was first extracted on mesh nodes in close proximity to the neck surface and then interpolated onto a uniform grid using the same procedure as for STAV. The time-average of the neck velocity was calculated and the maximum value of the time-averaged velocity was taken to be the 99th percentile. This value is referred to as MTAV and it was extracted pre- and post-treatment in order to calculate aneurysm neck MTAV reduction similarly to STAV reduction. We extracted the WSS field on the flow diverter surface in the post-treatment simulations and calculated STAWSS by taking the space-and-time-average of WSS across the entire clipped stent and all timesteps.

Our three primary variables of interest are aneurysm STAV reduction, neck MTAV reduction, and stent STAWSS. We performed a t-test for each variable with the null hypothesis that the independent samples (non-fetal and fetal) have identical means assuming identical variances. We calculated p -values and used a value of $p < 0.05$ to determine statistical significance. Each variable of interest was compared with the morphological quantities of interest, namely (i) aneurysm maximum diameter, (ii) aneurysm neck diameter, (iii) aneurysm aspect ratio, (iv) aneurysm non-sphericity index, and (v) PComA radius. We found a best-fit line for each data set and computed p and R^2 values. The occlusion rate in non-fetal and fetal groups was calculated using the $> 35\%$ STAV reduction haemodynamic end point for successful treatment. We tested alternative end point thresholds for STAV and MTAV, to determine the sensitivity of the results to this parameter.

2 Results

2.1 Outflow boundary condition sensitivity analysis

As well as the non-fetal and fetal PComA flow conditions (Supplementary Section 1.2), two additional boundary conditions are required at the MCA and ACA outlets. A simple choice for this is to use zero pressure outlets [14, 15, 16]. To investigate whether these simple outflow conditions are suitable for the FD-PComA IST, a sensitivity analysis was performed in one geometry. We imposed two sets of boundary conditions: (i) zero pressure conditions at the MCA and ACA; (ii) a mass flow condition at the MCA and a zero pressure condition at the ACA. In the latter case, we imposed a range of mass flow splits at the MCA (20%, 40%, 50%, 60%, 80%) and given that a mass flow condition was also imposed at the PComA, this ensures that the remainder of the flow passes down the ACA. For instance, when there is 80% of the MCA-ACA flow in the MCA, there will be 20% in the ACA.

For both sets of MCA-ACA boundary conditions, we performed pre- and post-treatment flow simulations under non-fetal and fetal PComA conditions and calculated the quantities of interest for the IST, namely the aneurysm STAV reduction, aneurysm neck MTAV reduction and the stent STAWSS. We then compared these quantities for the cases with the zero pressure conditions at both outlets to the cases with a mass flow condition applied to the MCA. The results are reported in Table 3. The percentage differences between the key quantities under both sets of boundary conditions are less than 0.1% in all cases. From this, we concluded that the outflow conditions applied at the MCA-ACA have a minimal impact on the results of the IST. As such, we opted to apply zero pressure outlet conditions at the MCA and ACA outlets.

Table 3: Two types of boundary conditions were applied to the MCA and the ACA and compared. The alternative MCA-ACA boundary conditions were to mass flow rate at the MCA. Given that a mass flow condition also applied at the PComA, the remainder of the flow at the MCA-ACA bifurcation therefore passes through the ACA. 20% MCA flow split therefore applies an 80% flow split through the ACA. The flow split MCA-ACA conditions were applied in one geometry for non-fetal and fetal PComA flow and three key flow variables (aneurysm STAV reduction, aneurysm neck MTAV reduction and stent STAWSS) were compared to the values obtained using zero pressure conditions applied at the MCA and ACA.

Non-fetal/fetal	MCA flow [%]	STAV reduction [%]	% difference in STAV reduction	MTAV reduction [%]	% difference in MTAV reduction	STAWSS [Pa]	% difference in STAWSS
<i>Zero pressure conditions</i>							
Non-fetal	NA	87.703	NA	69.542	NA	12.941	NA
Fetal	NA	40.191	NA	51.789	NA	18.159	NA
<i>Varying MCA-ACA flow split</i>							
Non-fetal	20.0	87.722	0.021	69.557	0.021	12.942	0.012
Non-fetal	40.0	87.711	0.009	69.549	0.009	12.940	0.006
Non-fetal	50.0	87.708	0.006	69.544	0.003	12.940	0.006
Non-fetal	60.0	87.707	0.005	69.544	0.003	12.941	0.002
Non-fetal	80.0	87.701	0.003	69.540	0.003	12.945	0.037
Fetal	20.0	40.219	0.070	51.784	0.009	18.161	0.012
Fetal	40.0	40.213	0.053	51.785	0.006	18.159	0.001
Fetal	50.0	40.214	0.056	51.787	0.002	18.158	0.001
Fetal	60.0	40.211	0.049	51.787	0.004	18.159	0.001
Fetal	80.0	40.191	0.001	51.791	0.005	18.161	0.011

ACA, anterior cerebral artery; MCA, middle cerebral artery; MTAV, maximum time-averaged velocity; STAV, space-and-time-averaged velocity; STAWSS, space-and-time-averaged wall shear stress.

2.2 Flow variables vs. morphological characteristics

Table 4 presents the R^2 and p values for the statistical tests performed between the haemodynamic parameters (aneurysm STAV reduction, aneurysm neck MTAV reduction and post-treatment stent STAWSS) and the morphological parameters (aneurysm maximum diameter, aspect ratio, neck width and non-sphericity index; PComA radius). The R^2 values describe the correlation between variables and the p values describe the suitability of a best fit linear regression applied to the data. The data and the lines of best fit are also plotted in Figures 2, 3, 4 and 5.

Table 4: Statistical values (R^2 and p value for best fit line) were calculated to quantify the correlation between flow variables (STAV/MTAV reduction, STAWSS) and morphological parameters (aneurysm maximum diameter, neck width, aspect ratio, NSI; PComA radius) for different physiologies (non-fetal, fetal, or both).

Morphological Variable	Flow Variable	Physiology and Statistics			
		Non-fetal		Fetal	
		R^2	p	R^2	p
Aneurysm max. diameter	STAV reduction	0.084	0.026	0.009	0.474
Aneurysm max. diameter	MTAV reduction	0.035	0.158	0.032	0.174
Aneurysm max. diameter	Stent STAWSS	0.015	0.354	0.001	0.806
Aneurysm aspect ratio	STAV reduction	0.009	0.482	0.001	0.772
Aneurysm aspect ratio	MTAV reduction	0.023	0.253	0.000	0.970
Aneurysm aspect ratio	Stent STAWSS	0.000	0.913	0.007	0.525
Aneurysm neck diameter	STAV reduction	0.209	0.000	0.008	0.506
Aneurysm neck diameter	MTAV reduction	0.042	0.121	0.046	0.104
Aneurysm neck diameter	Stent STAWSS	0.044	0.111	0.000	0.946
Aneurysm NSI	STAV reduction	0.004	0.634	0.006	0.548
Aneurysm NSI	MTAV reduction	0.001	0.793	0.000	0.918
Aneurysm NSI	Stent STAWSS	0.012	0.410	0.001	0.798
PComA radius	STAV reduction	0.021	0.279	0.023	0.257
PComA radius	MTAV reduction	0.002	0.734	0.112	0.009
PComA radius	Stent STAWSS	0.001	0.775	0.017	0.321

ICA, internal carotid artery; MTAV, aneurysm neck maximum time-averaged velocity; STAWSS, space-and-time-averaged wall shear stress; STAV, aneurysm space-and-time averaged velocity; PComA, posterior communicating artery.

2.2.1 Flow variables vs. PComA size

We plotted the three flow variables of interest (aneurysm STAV reduction, aneurysm neck MTAV reduction, stent STAWSS) against the size of the PComA vessel. PComA size was characterised by its radius. A line of best fit was found and the R^2 and p values for each plot were calculated. The R^2 values were small and the p values were large, demonstrating that there is not a significant relationship between any of the three flow variables or the two measures of PComA size.

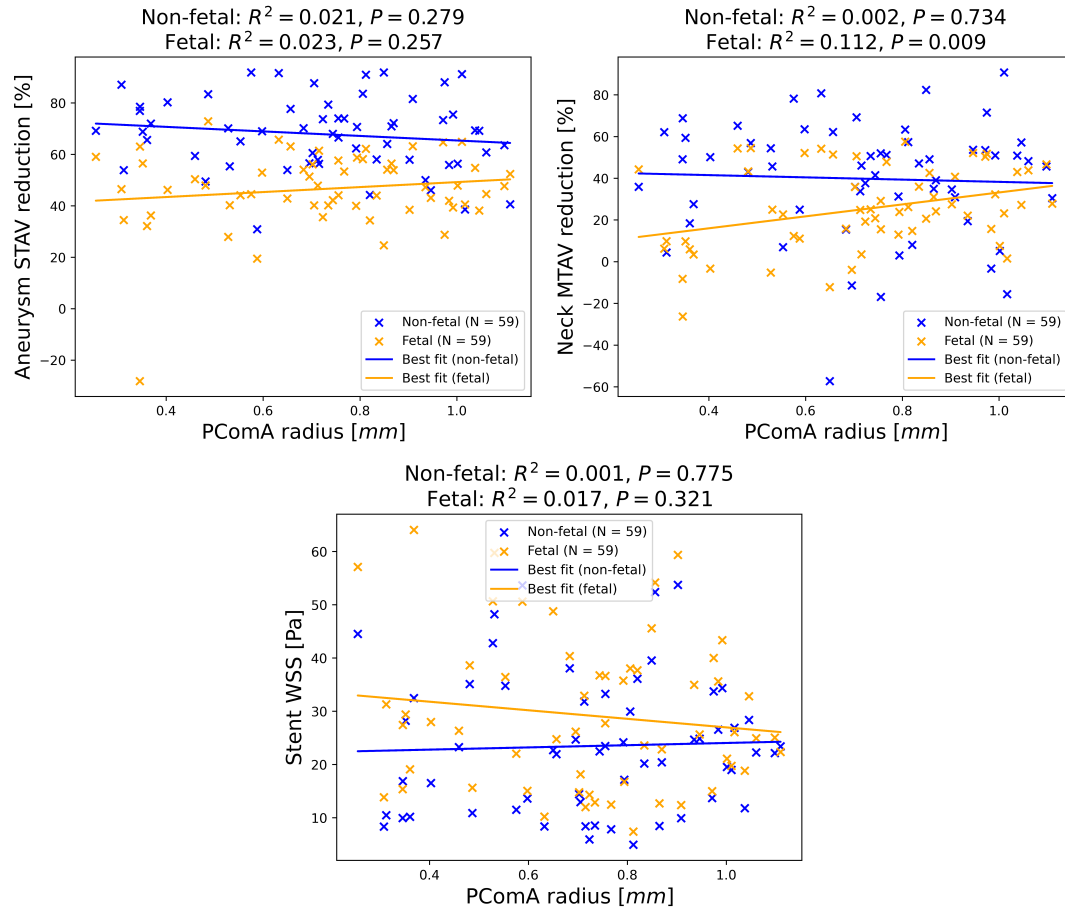


Figure 2: Flow variables vs. PComA size.

2.2.2 Flow variables vs aneurysm characteristics

We plotted the three flow variables of interest (aneurysm STAV reduction, aneurysm neck MTAV reduction, stent STAWSS) against four aneurysm morphological parameters (maximum diameter, neck diameter, aspect ratio, non-sphericity index). A line of best fit was found and the R^2 and p values for each plot were calculated. Figure 3 shows aneurysm STAV reduction against the morphological parameters. Figure 4 shows aneurysm neck MTAV against aneurysm morphology. Figure 5 shows stent STAWSS against aneurysm morphology. In each figure, the R^2 values are typically small and the p values are large. The lowest p value is found for aneurysm STAV reduction against aneurysm neck width ($p = 0.028$). These results suggest that aneurysm morphology typically does not play an important role in the assessment of treatment success using haemodynamic metrics.

Aneurysm STAV reduction

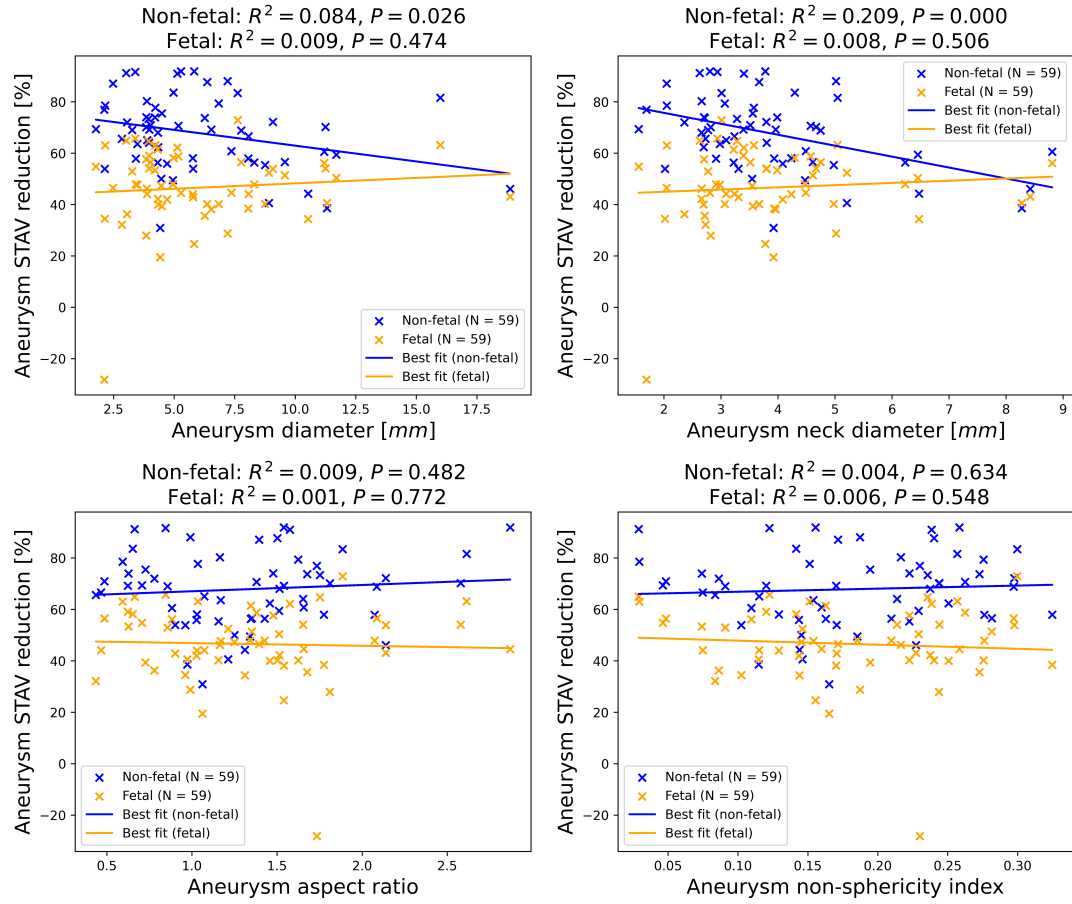


Figure 3: Aneurysm STAV vs aneurysm morphological characteristics.

Aneurysm neck MTAV reduction

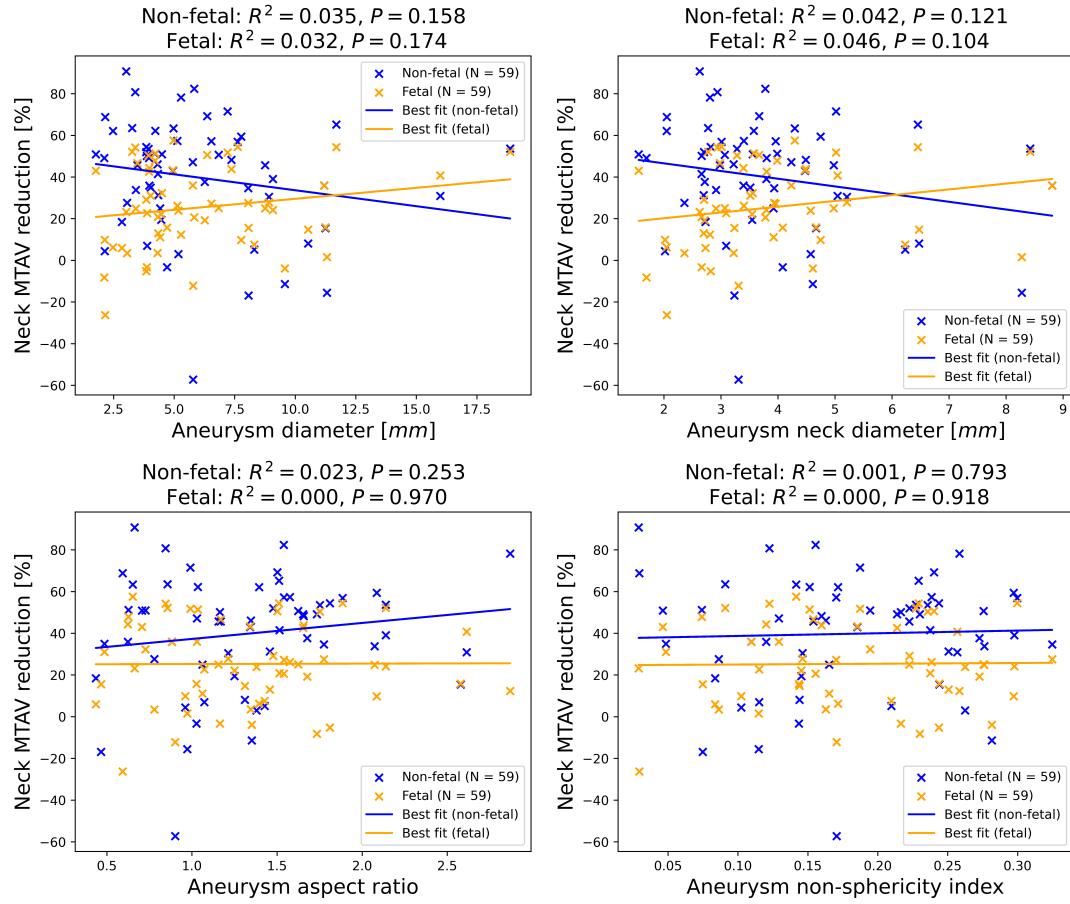


Figure 4: Aneurysm neck MTAV vs aneurysm morphological characteristics.

Stent STAWSS

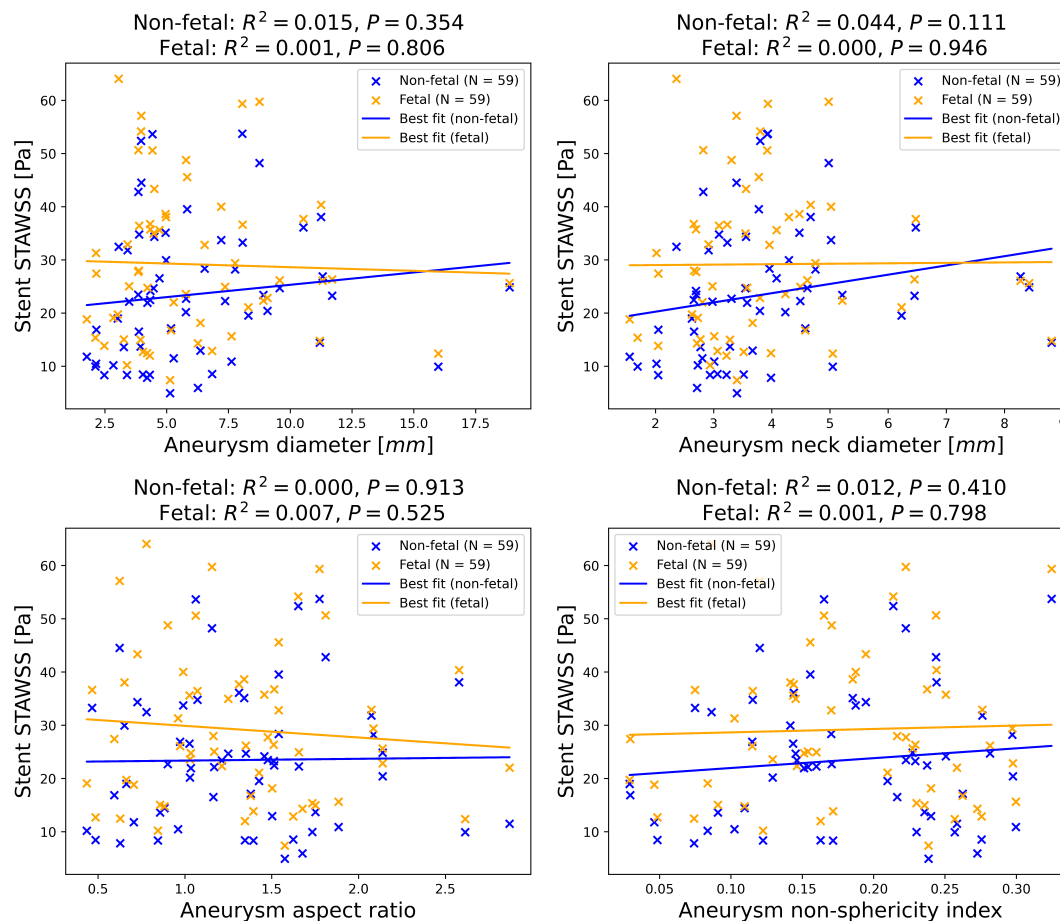


Figure 5: Stent STAWSS vs aneurysm morphological characteristics.

References

- [1] A Shaban, KC Albright, AK Boehme, S Martin-Schild, et al. Circle of willis variants: fetal pca. *Stroke Res Treat*, 2013, 2013.
- [2] F Lin, Y Xia, S Song, N Ravikumar, and AF Frangi. High-throughput 3DRA segmentation of brain vasculature and aneurysms using deep learning. *Comput Methods Programs Biomed*, 230:107355, 2023.
- [3] A Tagliasacchi, I Alhashim, M Olson, and H Zhang. Mean curvature skeletons. In *Computer Graphics Forum*, volume 31(5), pages 1735–1744. Wiley Online Library, 2012.
- [4] I Larrabide, M Kim, L Augsburger, MC Villa-Uriol, D Rufenacht, and AF Frangi. Fast virtual deployment of self-expandable stents: method and in vitro evaluation for intracranial aneurysmal stenting. *Med Image Anal*, 16(3):721–730, 2012.

- [5] S Appanaboyina, F Mut, R Löhner, C Putman, and J Cebal. Simulation of intracranial aneurysm stenting: techniques and challenges. *Comput Methods Appl Mech Eng*, 198(45-46):3567–3582, 2009.
- [6] A Sarrami-Foroushani, T Lassila, SM Hejazi, S Nagaraja, A Bacon, and AF Frangi. A computational model for prediction of clot platelet content in flow-diverted intracranial aneurysms. *J Biomech*, 91:7–13, 2019.
- [7] MD Ford, N Alperin, SH Lee, DW Holdsworth, and DA Steinman. Characterization of volumetric flow rate waveforms in the normal internal carotid and vertebral arteries. *Physiol Measur*, 26(4):477, 2005.
- [8] JPKH Alastruey, KH Parker, J Peiró, SM Byrd, and SJ Sherwin. Modelling the circle of willis to assess the effects of anatomical variations and occlusions on cerebral flows. *J Biomech*, 40(8):1794–1805, 2007.
- [9] L Zarrinkoob, K Ambarki, A Wählin, R Birgander, A Eklund, and J Malm. Blood flow distribution in cerebral arteries. *J Cereb Blood Flow Metab*, 35(4):648–654, 2015.
- [10] MC Villa-Uriol, G Berti, DR Hose, A Marzo, A Chiarini, J Penrose, J Pozo, JG Schmidt, P Singh, R Lycett, et al. @neurist complex information processing toolchain for the integrated management of cerebral aneurysms. *Interface Focus*, 1(3):308–319, 2011.
- [11] JR Cebal, MA Castro, S Appanaboyina, CM Putman, D Millan, and AF Frangi. Efficient pipeline for image-based patient-specific analysis of cerebral aneurysm hemodynamics: technique and sensitivity. *IEEE Trans Med Imaging*, 24(4):457–467, 2005.
- [12] J Ahrens, B Geveci, and C s Law. Paraview: An end-user tool for large data visualization. *The Visualization Handbook*, 717(8), 2005.
- [13] N Juchler, S Schilling, P Bijlenga, V Kurtcuoglu, and S Hirsch. Shape trumps size: image-based morphological analysis reveals that the 3D shape discriminates intracranial aneurysm disease status better than aneurysm size. *Front Neurol*, 13:809391, 2022.
- [14] A Sarrami-Foroushani, T Lassila, A Gooya, AJ Geers, and AF Frangi. Uncertainty quantification of wall shear stress in intracranial aneurysms using a data-driven statistical model of systemic blood flow variability. *J Biomech*, 49(16):3815–3823, 2016.
- [15] N Lv, Y Yu, J Xu, C Karmonik, J Liu, and Q Huang. Hemodynamic and morphological characteristics of unruptured posterior communicating artery aneurysms with oculomotor nerve palsy. *J of Neurosurg*, 125(2):264–268, 2016.
- [16] J Xu, Y Yu, X Wu, Y Wu, C Jiang, S Wang, Q Huang, and J Liu. Morphological and hemodynamic analysis of mirror posterior communicating artery aneurysms. *PLoS One*, 8(1):e55413, 2013.